JYX
JYVÄSKYLÄN YLIOPISTO
UNIVERSITY OF JYVÄSKYLÄ

This is a self-archived version of an original article. This version may differ from the original in pagination and typographic details.

Author(s): El-Naggar, Mostafa A.; Abu-Youssef, Morsy A. M.; Haukka, Matti; Barakat, Assem; Sharaf, Mona M.; Soliman, Saied M.

Title: Synthesis, X-ray Structure, and Hirshfeld Analysis of [Ag(3-amino-5,6-dimethyl-1,2,4-triazine)(NO3)]n : A Potent Anticancer and Antimicrobial Agent

Year: 2023

Version: Published version

Copyright: © 2023 the Authors

Rights: CC BY 4.0

Rights url: https://creativecommons.org/licenses/by/4.0/

Please cite the original version:

El-Naggar, M. A., Abu-Youssef, M. A. M., Haukka, M., Barakat, A., Sharaf, M. M., & Soliman, S. M. (2023). Synthesis, X-ray Structure, and Hirshfeld Analysis of [Ag(3-amino-5,6-dimethyl-1,2,4-triazine)(NO3)]n : A Potent Anticancer and Antimicrobial Agent. Inorganics, 11(9), Article 350. https://doi.org/10.3390/inorganics11090350

inorganics

MDPI

Article

Synthesis, X-ray Structure, and Hirshfeld Analysis of [Ag(3-amino-5,6-dimethyl-1,2,4-triazine)(NO_3)]$_n$: A Potent Anticancer and Antimicrobial Agent

Mostafa A. El-Naggar [1,*], Morsy A. M. Abu-Youssef [1], Matti Haukka [2], Assem Barakat [3], Mona M. Sharaf [4] and Saied M. Soliman [1,*]

[1] Department of Chemistry, Faculty of Science, Alexandria University, P.O. Box 426, Ibrahimia, Alexandria 21321, Egypt; morsy5@alexu.edu.eg
[2] Department of Chemistry, University of Jyväskylä, P.O. Box 35, FI-40014 Jyväskylä, Finland; matti.o.haukka@jyu.fi
[3] Department of Chemistry, College of Science, King Saud University, P.O. Box 2455, Riyadh 11451, Saudi Arabia; ambarakat@ksu.edu.sa
[4] Protein Research Department, Genetic Engineering and Biotechnology Research Institute, City of Scientific Research and Technological Applications, Alexandria P.O. Box 21933, Egypt; sharafmona4@gmail.com
* Correspondence: mostafa.elnaggar@alexu.edu.eg (M.A.E.-N.); saied1soliman@yahoo.com (S.M.S.)

Abstract: The [Ag(3ADMT)(NO_3)]$_n$ complex was synthesized by the self-assembly of 3-amino-5,6-dimethyl-1,2,4-triazine (3ADMT) and $AgNO_3$. Its molecular structure was analyzed utilizing FTIR spectra, elemental analysis, and single crystal X-ray diffraction (SC-XRD). There is one crystallographically independent Ag atom, which is tetra-coordinated by two nitrogen atoms from two 3ADMT and two oxygen atoms from two nitrate anions where all ligand groups are acting as connectors between the Ag1 sites. The geometry around the Ag(I) center is a distorted tetrahedron with a AgN_2O_2 coordination sphere augmented by strong argentophilic interactions between Ag atoms, which assist the aggregation of the complex units in a wavy-like and coplanar pattern to form a one-dimensional polymeric chain. The O...H (37.2%) and N...H (18.8%) intermolecular interactions contributed significantly to the molecular packing based on Hirshfeld surface analysis. The [Ag(3ADMT)(NO_3)]$_n$ complex demonstrates promising cytotoxicity against lung (IC_{50} = 2.96 ± 0.31 µg/mL) and breast (IC_{50} = 1.97 ± 0.18 µg/mL) carcinoma. This remarkable cytotoxicity exceeds those of 3ADMT, $AgNO_3$, and the anticancer medication *cis*-platin towards the tested cancer cell lines. In addition, the complex has a wide-spectrum antimicrobial action where the high antibacterial potency of the [Ag(3ADMT)(NO_3)]$_n$ complex against *P. vulgaris* (MIC = 6.1 µg/mL) and *B. subtilis* (MIC = 17.2 µg/mL) could be comparable to the commonly used drug Gentamycin (MIC = 4.8 µg/mL). These results confirm that the components of the [Ag(3ADMT)(NO_3)]$_n$ complex work together synergistically, forming a powerful multifunctional agent that could be exploited as an effective antimicrobial and anticancer agent.

Keywords: Ag(I); 1,2,4-triazine; coordination polymer; anticancer; antimicrobial; argentophilic interaction; Hirshfeld

check for updates

Citation: El-Naggar, M.A.; Abu-Youssef, M.A.M.; Haukka, M.; Barakat, A.; Sharaf, M.M.; Soliman, S.M. Synthesis, X-ray Structure, and Hirshfeld Analysis of [Ag(3-amino-5,6-dimethyl-1,2,4-triazine)(NO_3)]$_n$: A Potent Anticancer and Antimicrobial Agent. *Inorganics* **2023**, *11*, 350. https://doi.org/10.3390/inorganics11090350

Academic Editor: Peter Segl'a

Received: 9 August 2023
Revised: 21 August 2023
Accepted: 23 August 2023
Published: 25 August 2023

Copyright: © 2023 by the authors. Licensee MDPI, Basel, Switzerland. This article is an open access article distributed under the terms and conditions of the Creative Commons Attribution (CC BY) license (https://creativecommons.org/licenses/by/4.0/).

1. Introduction

The biological and pharmacological properties of silver(I) compounds attracted the attention of researchers working on coordination chemistry where numerous Ag(I) complexes had been proven to be anti-inflammatory, anti-tumor, or antibacterial compounds [1–10]. Particularly, the medicinal use of silver against local infections, whether in the form of inorganic salts or coordination compounds, is extensively approved [11,12]. Silver sulfadiazine (AgSD), for example, is a topical wide-spectrum drug used therapeutically for treating microbial infection in serious wounds or persistent burns [13–15]. The suggested mechanisms of silver complexes involve contact of Ag(I) ions with the cell membrane, enzyme

deactivation by interaction with thiol groups, association with DNA, and disruption of the electron transport chain [16–19]. The antimicrobial characteristics of silver(I) complexes are affected mainly by the type of atoms bound to the silver metal and the feasibility of ligand substitution. Silver(I) complexes with a greater possibility of ligand substitution by biologically active ligands (sulphur compounds) exhibit a stronger antimicrobial action. As a result, complexes having weak Ag–O and Ag–N bonds showed a wider spectrum of antibacterial behavior than Ag-S species. Practically, all Ag–P bound compounds have exhibited little or no action towards yeast, bacteria, or molds [5,6,8,20,21].

Triazine derivatives have been approved to have a wide range of therapeutic activity [22–24] with particular attention to their antiviral [25], antimicrobial [22–24], anticancer [26,27], and antifungal [28] activities. Drugs with 1,2,4-triazine moiety were found in many synthetic and natural products, such as lamotrigine and azaribine, which have significant pharmacological effects [29]. Also, there are several examples of biologically active complexes with triazine ligands [30–34]. Previous studies [35,36] showed that the addition of planar-condensed aromatic ligands containing nitrogen (whose donor characteristics are similar to those of pyrimidine and purine bases) to anti-tumor agents leads to intriguing features that can be used to create new drugs. This promotes the formation of complexes with DNA subunits, which is a main objective in tumor treatment [37].

In this context, looking for promising metal-based compounds, which can be utilized as anticancer and antimicrobial drugs, is necessary. Special interest in discovering metal-based antibiotics is caused by the increase in the strains that are resistant to commonly used organic antibiotics and the problems in treating their infections [38]. It was acknowledged that the biologically active ligand would work in a synergistic manner in coordination connection with the Ag(I) ion [33]. From this point of view, we present in this work the synthesis, structure analyses, and in vitro anticancer, antibacterial, and antifungal properties of a newly synthesized silver complex based on 3-amino-5,6-dimethyl-1,2,4-triazine (3ADMT) (Figure 1).

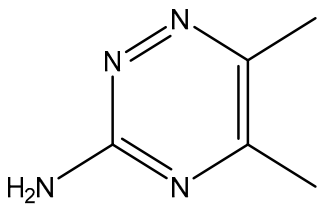

Figure 1. Structure of 3-Amino-5,6-dimethyl-1,2,4-triazine (3ADMT).

2. Results and Discussion

2.1. Synthetic Strategy

In our recent study [33], we presented the synthesis and biological activity of $[Ag_2(2ClDAT)_2(NO_3)_2(H_2O)]_n$ where 2ClDAT is 2-chloro-4,6-diamino-1,3,5-triazine. This complex was prepared by self-assembly of 2ClDAT with silver nitrate. In extension to this study, the self-assembly of the organic ligand 3-amino-5,6-dimethyl-1,2,4-triazine (3ADMT) and $AgNO_3$ leads to the formation of a new crystalline silver(I) complex. 3ADMT is a good candidate because it has a triazine ring, which has the ability to coordinate the metal ion, and its amino and methyl groups can make inter- or intramolecular hydrogen bonding with other hydrogen bond acceptors. Also, the silver salt, $AgNO_3$, was selected as an inorganic unit because it possesses the self-assembly capability to form a supramolecular complex through its bridging nitrate anion. These fragments can be linked together to form polymeric organic–inorganic hybrid architecture in which both the nitrate groups and the organic unit (3ADMT) act as bridging ligands, enhancing the stability of the crystalline polymeric silver(I) compound. The structure of the new complex has been confirmed by elemental analysis, infrared spectra, and SC-XRD to be $[Ag(3ADMT)(NO_3)]_n$.

2.2. X-ray Structural Analysis of $[Ag(3ADMT)(NO_3)]_n$

The complex $[Ag(3ADMT)(NO_3)]_n$ crystallizes in the monoclinic space group $P2_1/n$ with Z = 4 and one monomer $[Ag(3ADMT)(NO_3)]$ as an asymmetric unit. The crystal refinement information is scheduled in Table S1, Supplementary data. The unit cell parameters are a = 12.2062(2) Å, b = 5.07870(10) Å, c = 15.0031(3) Å, and β = 108.832(2)° while V= 880.28(3) Å^3. Figure 2 displays the scheme of the atom numbering and coordination geometry of this complex. The monomeric unit consists of one organic ligand per $AgNO_3$.

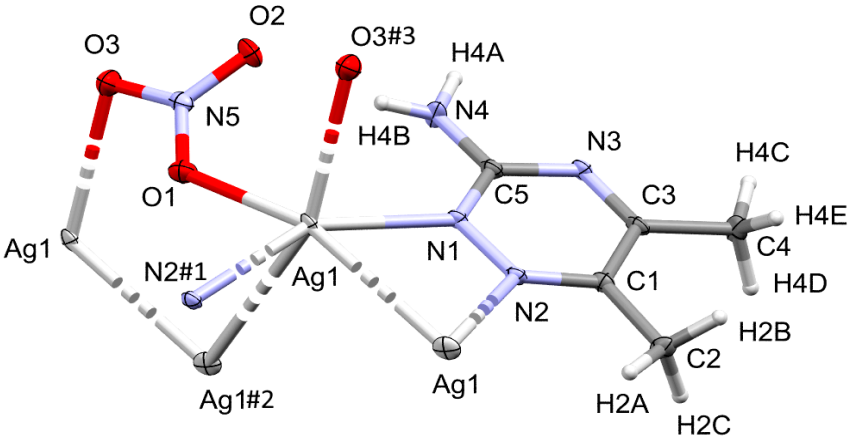

Figure 2. Drawing of displacement ellipsoids (50% probability) of $[Ag(3ADMT)(NO_3)]_n$, showing the atom-numbering scheme. The bonds, Ag1–N2#1, Ag1–Ag1#2, and Ag1–O3#3, are displayed with a broken line, as the N2#1, Ag1#2 and O3#3 atoms are a part of the adjacent monomers, however they remain in the silver atom's coordination sphere. The symmetry for N2#1, Ag1#2 and O3#3 are #1: 1/2 – x, 1/2 + y, 3/2 – z, #2: 1/2 – x, y – 1/2, 3/2 – z, and #3: x, −1 + y, z, respectively.

In this Ag(I) complex, there is one crystallographically independent Ag atom, which is tetra-coordinated by two N-atoms from two 3ADMT and two O-atoms from two nitrate groups where all ligands groups act as linkers between the Ag(1) centers. Table 1 presents selected interatomic distances and bond angles. The distances of the coordinate bonds Ag1–N1, Ag1–N2#1 (Symm. code: #1 1/2 − x, 1/2 + y, 3/2 − z), Ag1–O1, and Ag1–O3#3 (Symm. code: #3 x, −1 + y, z) are 2.2330(16), 2.2634(15), 2.4386(18), and 2.6293(17) Å, respectively. The N1–Ag1–N2#1 (Symm. code: #1 1/2 − x, 1/2 + y, 3/2 − z) and O1–Ag1–O3#3 (Symm. code: #3 x, −1 + y, z) angles are 149.29(6)° and 94.71(6)°, respectively. As a result, the coordination geometry of silver(I) in the complex could be described as a distorted tetrahedral augmented by argentophilic interactions, by which the silver atoms are connected in a coplanar and wavy-like manner to create a one-dimensional polymeric chain. The Ag1−Ag1#2 (Symm. code: #2 1/2 − x, y − 1/2, 3/2 − z) bond length is 3.2263(2) Å. This distance is quite short, representing a notable argentophillic interaction [39] that causes the 1D polymer to expand across the crystallographic b-axis (Figure 3). In addition to these argentophilic interactions, this polymeric sequence is further connected via the bridging of nitrate groups, which has a significant impact on the polymer expansion. As shown in Figure 3, the nitrate anion serves as a linker between the Ag(I) centers through Ag1–O1 and Ag1–O3 bonds along both sides around the Ag–Ag bonds. The organic ligand, 3-amino-5,6-dimethyl-1,2,4-triazine, is also acting as a bridging ligand, which is coordinated via its neighboring two nitrogen atoms, N1 and N2, to successive silver atoms, Ag1 and Ag1#2 (Symm. code: #2 1/2 − x, y − 1/2, 3/2 − z), linked by the argentophilic interactions, forming a trapezoid structure in which the two silver atoms construct the longer base and the two nitrogen atoms form the shorter base. The ligand units are arranged in an alternative pattern above and below the polymer array.

Table 1. Bond distances [Å] and angles [°] for $[Ag(3ADMT)(NO_3)]_n$.

Bond	Distance	Bond	Distance
Ag(1)–N(1)	2.2330(16)	Ag(1)–Ag(1)#2	3.2263(2)
Ag(1)–N(2)#1	2.2634(15)	Ag(1)–O(1)	2.4386(18)
Ag1–O3#3	2.6293(17)		
Bonds	Angle	Bonds	Angle
N(1)–Ag(1)–N(2)#1	149.29(6)	O(1)–Ag(1)–Ag(1)#2	163.69(4)
N(1)–Ag(1)–O(1)	123.44(6)	N(1)–Ag(1)–Ag(1)#1	107.10(4)
N(2)#1–Ag(1)–O(1)	80.87(6)	N(2)#1–Ag(1)–Ag(1)#1	65.83(4)
N(1)–Ag(1)–Ag(1)#2	65.08(4)	O(1)–Ag(1)–Ag(1)#1	61.23(4)
N(2)#1–Ag(1)–Ag(1)#2	86.97(4)		

Symm. codes: #1: −x + 1/2, y + 1/2, −z + 3/2 #2: −x + 1/2, y − 1/2, −z + 3/2, and #3: x, −1 + y, z.

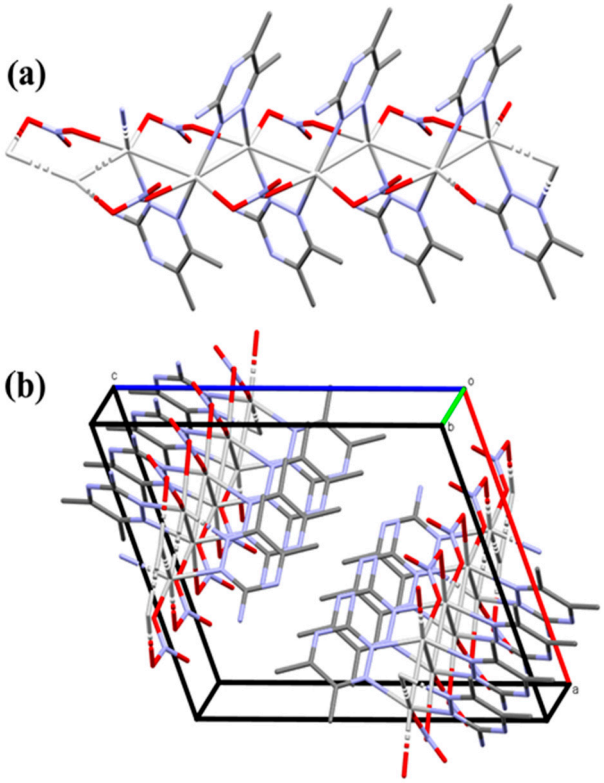

Figure 3. The 1D infinite coordination polymer of $[Ag(3ADMT)(NO_3)]_n$ complex (part **a**) and the projections of the polymeric chains in the unit cell (part **b**). All hydrogen atoms are removed for better visualization.

In contrast, the silver(I) ion is found coordinated to three triazine molecules forming a nearly regular trigonal–planar geometry in the structurally related $[Ag(3ADMT)_3](CF_3O_3S)(3ADMT)$ monomeric complex [40]. Also, unlike the studied complex, the $[Ag(3ADMT)_3](CF_3O_3S)(3ADMT)$ complex is not a coordination polymer where the organic ligand acts as a monodentate terminal ligand instead of a linker between the silver centers. In addition, the trifluoromethane sulfonate anion, unlike the bridging nitrate group, is freely uncoordinated. In comparison to $[Ag(3ADMT)(NO_3)]_n$, the N–Ag–N angles in $[Ag(3ADMT)_3](CF_3O_3S)(3ADMT)$ complex are smaller (118.6(2)–121.8(3)°) indicating approximately planar coordination environment around the silver center. On the other hand, the Ag–N bond distances (2.241(6)–2.273(6) Å) are close to those found in the $[Ag(3ADMT)(NO_3)]_n$ complex.

With regard to the crystal structure packing, there is N4-H4B...O2 intramolecular hydrogen bonding, which is displayed in the light blue dotted line in Figure 4A, with H...O distance of 2.064(3) Å. In addition, numerous intermolecular O. . .H and N. . .H (shown in

red) interactions link the units with each other in the polymer chain (Figure 4B). Details concerning these interactions are set in Table 2.

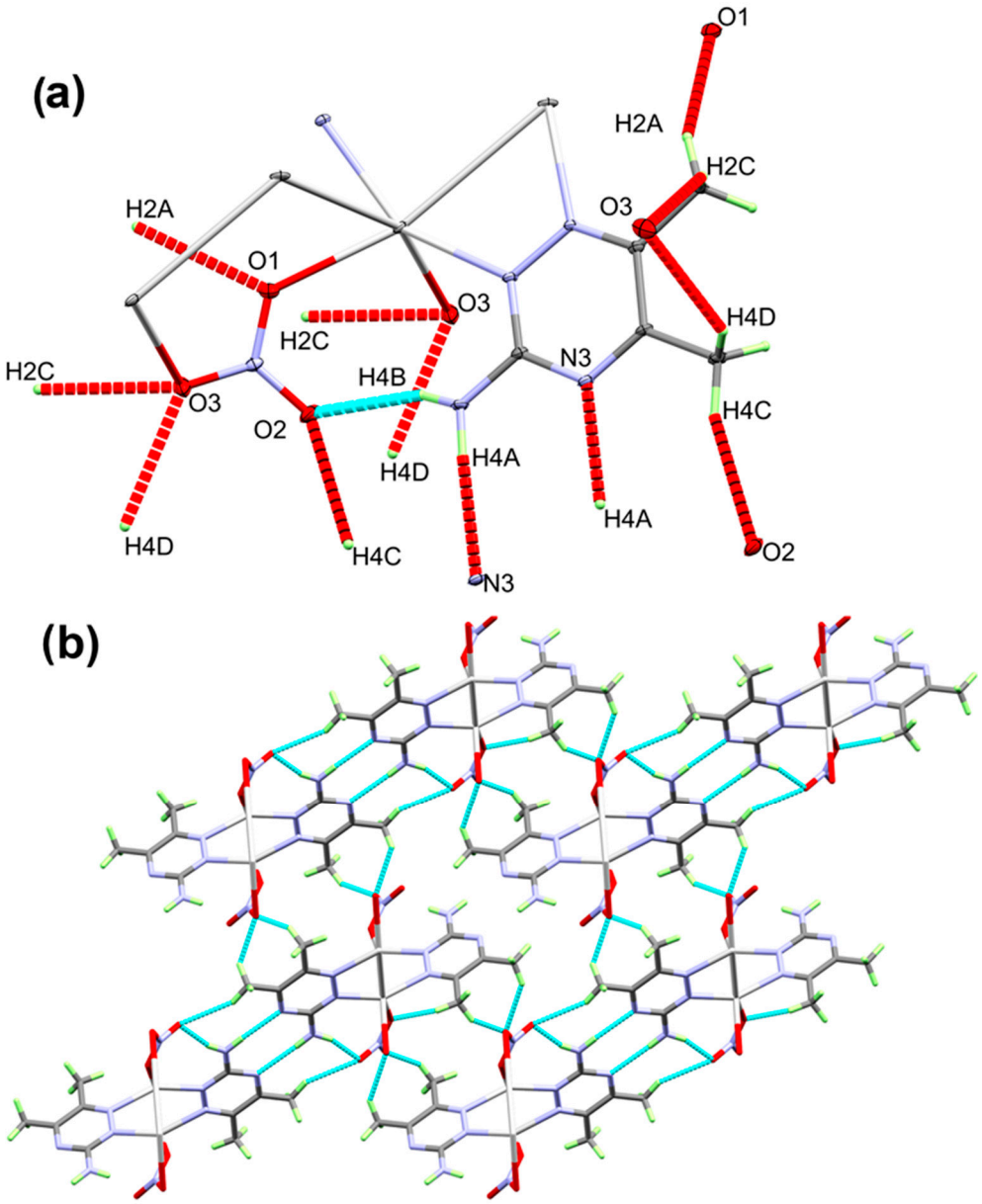

Figure 4. The O. . .H and N. . .H contacts (part **a**) and the packing view along *ac* plane (part **b**) for the $[Ag(3ADMT)(NO_3)]_n$ complex.

Table 2. The important intermolecular interactions [Å and °] for $[Ag(3ADMT)(NO_3)]_n$.

D-H...A	d(D-H)	d(H...A)	d(D...A)	<(DHA)	Symmetry Codes
N4-H4B...O2	0.84(3)	2.064(3)	2.848(3)	154.8	
C2-H2A. . .O1	0.98	2.503	3.413(3)	154.3	1/2 − x, −3/2 + y, 3/2 − z
C2-H2C. . .O3	0.98	2.460	3.259(2)	138.5	−1/2 + x, 3/2 − y, −1/2 + z
C4-H4C. . .O2	0.98	2.547	3.454(3)	153.8	1 − x, 1 − y, 1 − z
C4-H4D. . .O3	0.98	2.534	3.321(3)	137.3	−1/2 + x, 3/2− y, −1/2+z
N4-H4A. . .N3	0.89(3)	2.16(3)	3.052(3)	176(3)	1 − x, 1 − y, 1 − z

On the other hand, the parallel chains in the crystal structure are packed together via O2. . .H4C (2.549 Å) and N3. . .H4A (2.163 Å) interactions. The uncoordinated oxygen atom (O2) of the nitrate anions interacts with the hydrogen atoms of the methyl groups

connecting the chains via C-H. . .O interactions. Additionally, the freely uncoordinated nitrogen atoms share in the crystal packing by linking the chains via N...H hydrogen bonds (Figure 5).

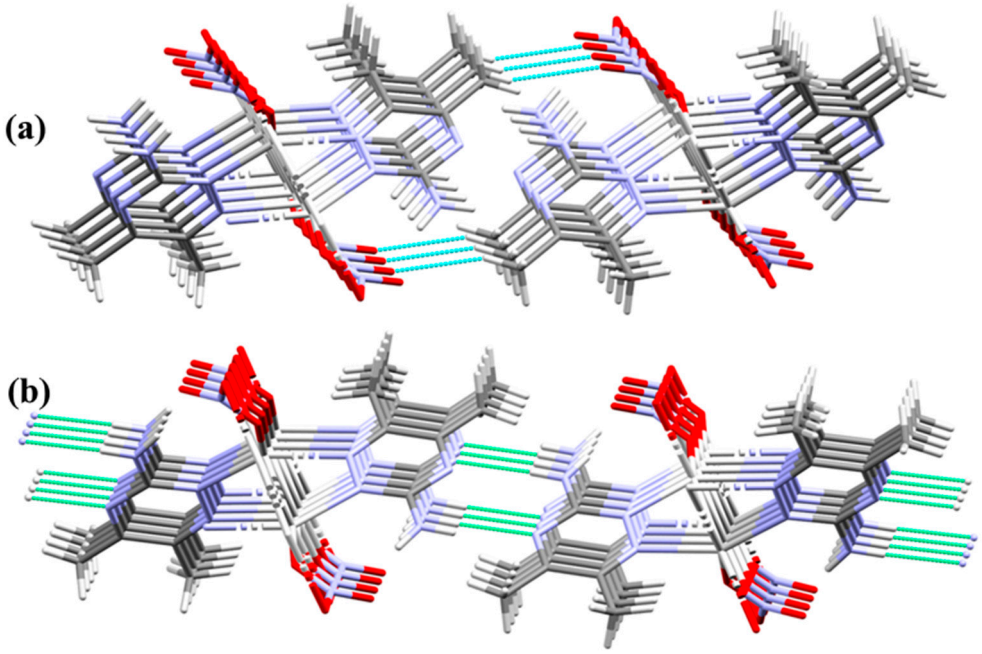

Figure 5. Packing of the polymeric chains via O. . .H (part **a**) and N. . .H (part **b**) interactions.

The X-ray structure of the structurally comparable $[Ag_2(2ClDAT)_2(NO_3)_2(H_2O)]_n$ complex revealed a 1D coordination polymer through the NO_3^- group as a linker between silver(I) centers [33] but in the case of $[Ag(3ADMT)(NO_3)]_n$, the polymeric chain is further supported by Ag–Ag bonds.

2.3. FTIR Spectra

The infrared spectral analysis of the $[Ag(3ADMT)(NO_3)]_n$ complex and its free ligand, 3ADMT, were recorded and displayed in Figures S1 and S2 (Supplementary data). The FTIR spectrum of the complex matches that of the free ligand except for the presence of a very sharp spectral band in the FTIR spectrum of the $[Ag(3ADMT)(NO_3)]_n$ complex at 1385 cm^{-1} confirming the existence of the NO_3^- group. In the infrared spectra of the $[Ag(3ADMT)(NO_3)]_n$ complex and its ligand, the peaks appearing in the range 3097–2920 cm^{-1} could be attributed to the C(sp^3)-H stretching vibrations of the methyl groups. In addition, the peaks in the range 1667–1668 and 1563–1564 cm^{-1} could be attributed to the υ(C=N) and υ(C=C) stretching modes of the triazine moiety, respectively. Furthermore, there are strong bands in the range of 3284–3188 cm^{-1} corresponding to $\upsilon(NH_2)$ stretching vibrational modes.

2.4. Hirshfeld Surface Analysis

The molecules in the crystal are packed together to enhance crystal stability through a combination of intermolecular contacts. The Hirshfeld surface is a geometrical model utilized in supramolecular structure description to explain the packing and intermolecular contacts in the crystalline compounds [41]. The surface of Hirshfeld is the outermost boundary of the area where the studied molecule resides after it is crystallized [42–44]. The percentages of all potential intermolecular contacts in the crystal structure of $[Ag(3ADMT)(NO_3)]_n$ are computed using fingerprint (FP) plots and summarized in Figure 6, which reveals that the O. . .H (37.2%), H. . .H (21.5%), N. . .H (18.8%), and C. . .H (6.5%) are the most abundant interactions.

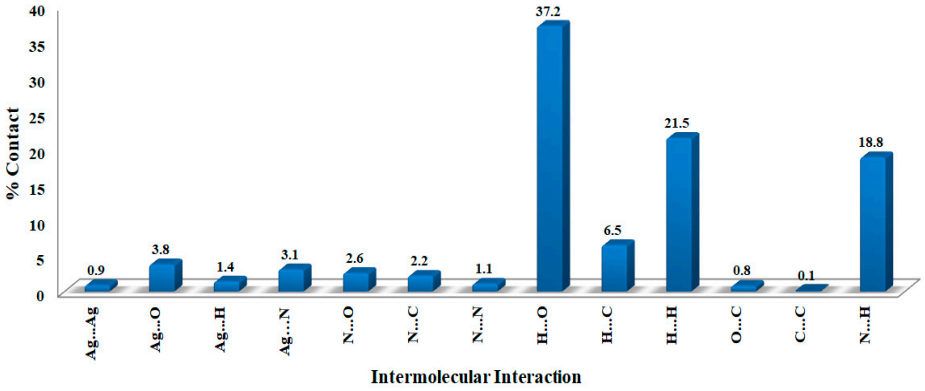

Figure 6. The contributions of all intermolecular interactions in the $[Ag(3ADMT)(NO_3)]_n$ complex.

The different Hirshfeld surfaces (d_{norm}, curvedness, and shape index) of the $[Ag(3ADMT)(NO_3)]_n$ complex are displayed in Figure S3. In the upper part of Figure S3, the d_{norm} map reveals the existence of numerous intense red spots that correspond to the most significant intermolecular interactions. The bright red spots designated as A in the d_{norm} map found adjacent to the central Ag(I) could be attributed to the coordination interactions with the organic ligand and the bridged nitrato group in addition to the argentophilic interaction. The %Ag–N, %Ag–O, and %Ag–Ag contacts are 3.1, 3.8, and 0.9%, respectively. Additionally, the bridged nitrato and the argentophilic interactions have an important role in the 1D polymer extension (Figure 7). It is obvious from the d_{norm} maps that the Ag–O and Ag–Ag interactions are displayed as intense red spots, as demonstrated in Figure 7, which confirms the polymeric structure of this complex.

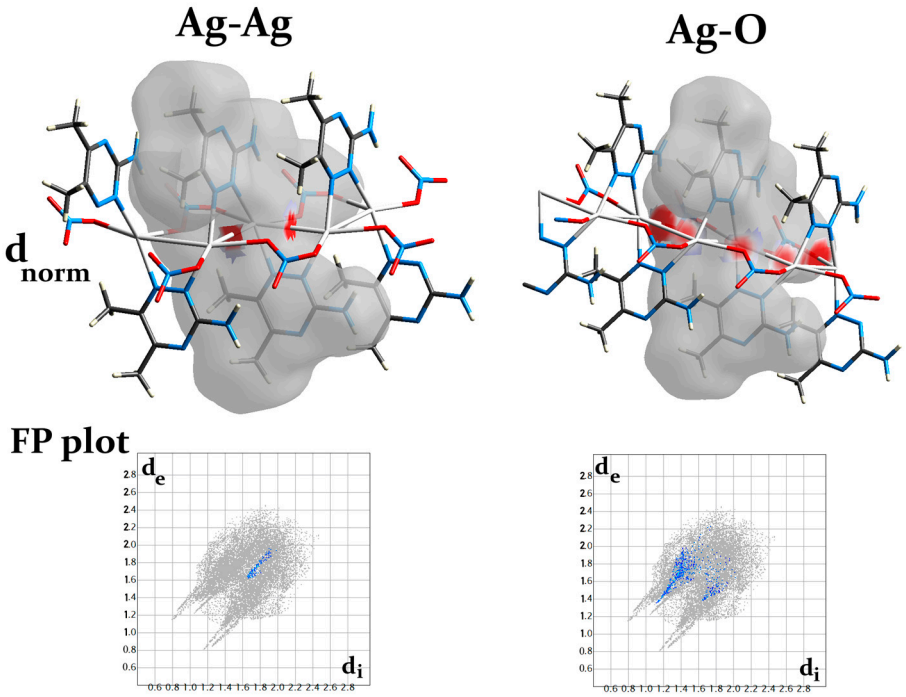

Figure 7. The d_{norm} surface and fingerprint (FP) plots of the Ag–O and Ag–Ag interactions.

As noted from Figure 8, the O. . .H and N...H contacts participated significantly in the crystal packing and were important for the crystal stability, since the polymeric chains are interconnected by these hydrogen bonds. The d_{norm} surfaces and fingerprint (FP) plots of the O...H and N...H interactions showed intense, large red spots and sharp spikes, respectively (Figure 9).

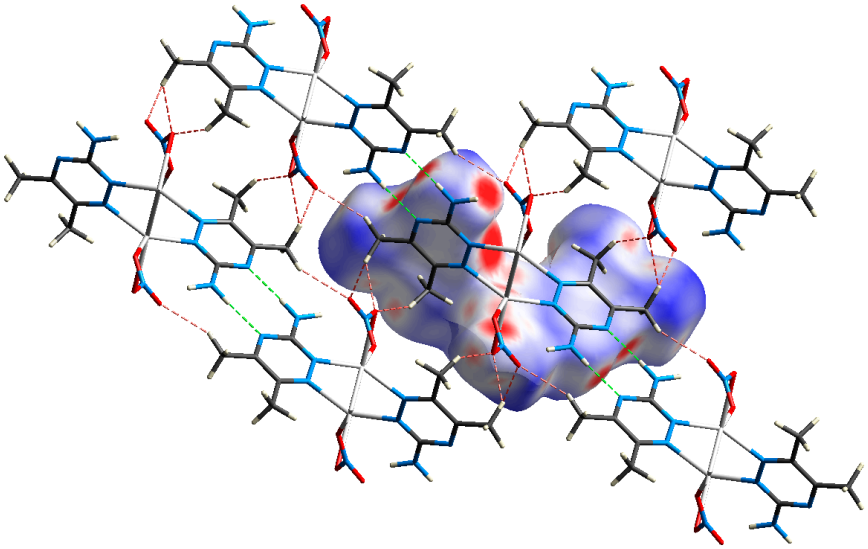

Figure 8. Crystal packing of the complex via hydrogen bonds, O…H (red) and N…H (green) interactions.

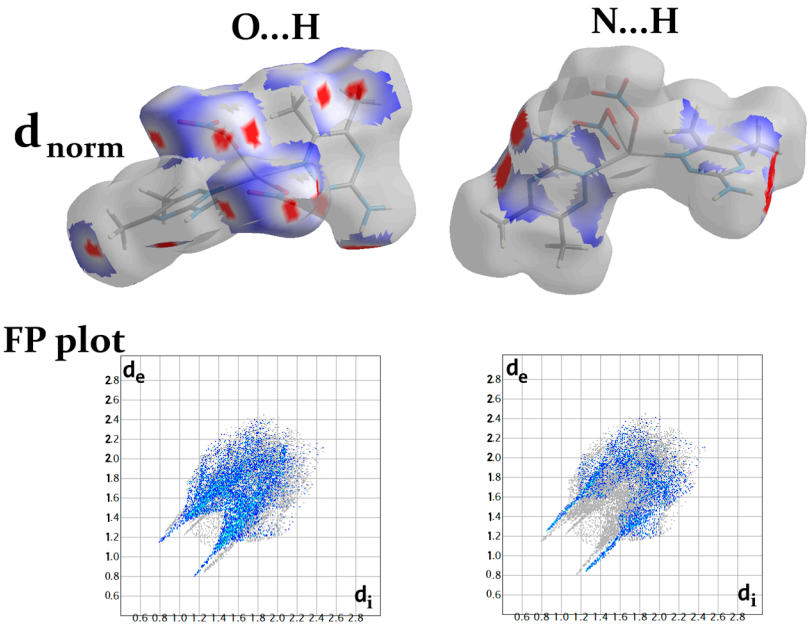

Figure 9. The d_{norm} surface and fingerprint plots of the O…H and N…H interactions.

2.5. Cytotoxic Potential

The MTT method was applied to evaluate the in vitro cytotoxicity of the $[Ag(3ADMT)(NO_3)]_n$ complex as IC_{50} values in µg/mL against two human cancerous cell lines, lung (A-549) and breast (MCF-7) carcinoma. The comprehensive findings are listed in Tables S2–S5 (Supplementary data) and visually displayed in Figure S4. A summary of these outcomes is presented in Table 3. The IC_{50} values of the $[Ag(3ADMT)(NO_3)]_n$ complex are compared to the free 3ADMT and $AgNO_3$ as well as *cis*-platin as a positive control. *Cis*-platin is one of the most potent anticancer medicines currently in use [45]. However, its narrow spectrum of activity and unfavorable side effects, such as neurotoxicity, nausea, nephrotoxicity vomiting, and myelo-suppression [46–48], which restrict the dose that can be administered to patients, limit its therapeutic utility [49]. To avoid these disadvantages, researchers have studied a novel family of metal-containing drugs that are less toxic and more effective. Ag(I) complexes have grown in prominence in recent years as anticancer therapeutics with negligible toxicity to healthy human cells [1,2,4,7,50–54].

Table 3. IC_{50} values (in μg/mL) for $[Ag(3ADMT)(NO_3)]_n$, $[Ag_2(2ClDAT)_2(NO_3)_2(H_2O)]_n$, 3ADMT, $AgNO_3$, and *cis*-platin towards particular cancerous cell lines.

Compound	A-549	MCF-7
$[Ag(3ADMT)(NO_3)]_n$	2.96 ± 0.31	1.97± 0.18
$[Ag_2(2ClDAT)_2(NO_3)_2(H_2O)]_n$	1.85 ± 0.26	3.01 ± 0.59
3ADMT	239.66 ± 6.28	214.21 ± 5.97
$AgNO_3$	14.70 ± 0.53	2.81 ± 0.97
cis-platin	7.5 ± 0.69	4.59 ± 0.53

As shown in Table 3, the $[Ag(3ADMT)(NO_3)]_n$ complex demonstrates promising and greater cytotoxicity than 3ADMT and $AgNO_3$ towards the examined cancerous cell lines. The cytotoxic activity of the free ligand is small (IC_{50} > 200 μg/mL) compared to the $[Ag(3ADMT)(NO_3)]_n$ complex. In contrast, the IC_{50} values of the $[Ag(3ADMT)(NO_3)]_n$ complex are 2.96 ± 0.31 and 1.97 ± 0.18 μg/mL towards A-549 and MCF-7 cell lines, respectively. In comparison with the related Ag(I) complex $[Ag_2(2ClDAT)_2(NO_3)_2(H_2O)]_n$ [33], the cytotoxicity of $[Ag(3ADMT)(NO_3)]_n$ is greater than that of $[Ag_2(2ClDAT)_2(NO_3)_2(H_2O)]_n$ in the case of breast carcinoma (MCF-7) while the opposite is true in the case of lung carcinoma (A-549). Generally, both complexes exhibited higher cytotoxicity against the two cell lines than *cis*-platin (Table 3). Based on the IC_{50} values of the $[Ag(3ADMT)(NO_3)]_n$ and $[Ag_2(2ClDAT)_2(NO_3)_2(H_2O)]_n$ complexes, the silver complexes with triazine ligands could have a great importance as anticancer drugs in the near future.

2.6. Antimicrobial Activity

The antimicrobial characteristics of Ag(I) complexes containing several *N*-heterocycles have received approval [3,8,54–56]. In this context, the antimicrobial activities of the investigated complex were assessed in terms of Minimum Inhibition Concentrations (MIC) and inhibition zone diameters against six microbial microorganisms. The results were compared to those of other marketed antibiotics such as Gentamycin and Ketoconazole under the same conditions. The microbes used in this study are two Gram-positive bacteria (*St. aureus* and *B. subtilis*), two Gram-negative bacteria (*E. coli* and *P. vulgaris*), and two fungi (*A. fumigatus* and *C. albicans*). It is observed from Table 4 that 3ADMT is ineffective towards all examined microbes. On the contrary, its Ag(I) complex $[Ag(3ADMT)(NO_3)]_n$ has wide-spectrum action against all tested microorganisms except *A. fumigatus*. This may provide insight into how bioactivity increases when Ag(I) is introduced.

Table 4. Inhibition zone diameters (mm) and MIC (μg/mL) values for the studied complex $[Ag(3ADMT)(NO_3)]_n$, free ligand 3ADMT, $AgNO_3$, $[Ag_2(2ClDAT)_2(NO_3)_2(H_2O)]_n$, and commercial antibiotics [a].

Compound	Gram-Positive Bacteria		Gram-Negatvie Bacteria		Fungi	
	St. aureus	*B. subtilis*	*E. coli*	*P. vulgaris*	*A. fumigatus*	*C. albicans*
$[Ag(3ADMT)(NO_3)]_n$	15 (30.5)	17 (17.2)	16 (30.5)	22 (6.1)	NA[d] (ND [e])	15 (156.25)
$[Ag_2(2ClDAT)_2(NO_3)_2(H_2O)]_n$	12 (156)	13 (156)	9 (625)	14 (312.5)	NA[d] (ND [e])	NA[d] (ND [e])
$AgNO_3$	14 (64)	13 (312.5)	15 (32)	20 (156)	NA[d] (ND [e])	10 (128)
3ADMT	NA[d] (ND [e])	NA[d] (ND [e])	NA[d] (ND [e])	NA[d] (ND [e])	NA[d] (ND [e])	NA[d] (ND [e])
Control	24 (9.7) [b]	26 (4.8) [b]	30 (4.8) [b]	25 (4.8) [b]	17 (156.25) [c]	20 (312.5) [c]

[a] MIC values are in parentheses; [b] Gentamycin; [c] Ketoconazole; [d] NA: no activity; and [e] ND: not determined.

Furthermore, the $[Ag(3ADMT)(NO_3)]_n$ outperformed $AgNO_3$ and the previously prepared $[Ag_2(2ClDAT)_2(NO_3)_2(H_2O)]_n$ in terms of antibacterial and antifungal properties. Interestingly, the studied silver(I) complex has remarkable antibacterial potential against *P. vulgaris* (MIC = 6.1 μg/mL) and *B. subtilis* (MIC = 17.2 μg/mL), which could be comparable to Gentamycin (MIC = 4.8 μg/mL for both bacteria). On the other hand,

both silver(I) complexes, $AgNO_3$, and the free ligand do not have any antifungal potential against *A. fumigatus*. Also, the inhibition zone diameters are in accordance with the MIC values, supporting the wide-spectrum antibacterial action of the investigated complex.

3. Materials and Methods

3.1. Chemicals and Physicochemical Characterizations

All chemicals were purchased from Sigma-Aldrich Company Inc. (St. Louis, MO, USA). The FTIR analyses were performed at 4000–400 cm^{-1} by utilizing a Bruker Tensor 37 FTIR equipment (Bruker, Germany) in potassium bromide pellets. The CHN analysis was performed by using Perkin Elmer 2400 Elemental Analyzer (PerkinElmer Inc., Waltham, MA, USA). A Shimadzu atomic absorption spectrophotometer (AA-7000 series, Shimadzu, Ltd., Tokyo, Japan) was utilized to determine the amount of silver present. Shimadzu atomic absorption spectrophotometer (AA-7000 series, Shimadzu, Ltd., Japan).

3.2. Synthesis of [Ag(3ADMT)(NO_3)]$_n$

An aqueous solution (10 mL) of $AgNO_3$ (170 mg, 1 mmol) was mixed with an ethanolic solution of 3ADMT (124.14 mg, 1 mmol). This mixture results in the formation of a precipitate that dissolves well in acetonitrile. At 25 °C, this clear solution was left to be evaporated gently. The $[Ag(3ADMT)(NO_3)]_n$ was generated as transparent crystals within a few days. The acquired crystals were appropriate for single crystal X-ray measurements.

$[Ag(3ADMT)(NO_3)]_n$; (73% yield). Anal. Calc. $C_5H_8AgN_5O_3$: C, 20.42; H, 2.74; N, 23.82; and Ag, 36.69%. Found: C, 20.31; H, 2.70; N, 23.61; and Ag, 36.94%. FTIR cm^{-1}: 3283, 3188, 3097, 2994, 2922, 1668, 1564, 1487, 1385, 1138, 1103, 1012, 949, 792, 633, and 533. 3ADMT: 3284, 3189, 3091, 2993, 2920, 1667, 1563, 1484, 1138, 1102, 1012, 948, 794, 634, and 532 (Figures S1 and S2, Supplementary data).

3.3. Crystal Structural Analysis

X-ray structure measurement and instrumental details are demonstrated in Supplementary data [57–60]. The crystal information of the silver(I) complex is shown in Table S1.

3.4. Hirshfeld Surface Analysis

Crystal Explorer Ver. 3.1 [61] program package was used to generate the 2D fingerprint plots and study the Hirshfeld surfaces.

3.5. Assessment of Cytotoxic and Antimicrobial Activities

The cytotoxic efficacy of the $[Ag(3ADMT)(NO_3)]_n$ complex towards the lung (A-549) and breast carcinoma (MCF-7) cell lines was investigated utilizing the technique outlined in Method S1 (Supplementary data) [62]. The antimicrobial effectiveness of the Ag(I) complex and its ligand against Gram-positive, Gram-negative bacteria, and pathogenic fungi was assessed. Method S2 (Supplementary data) contains more information.

4. Conclusions

In this study, the structure of the polymeric complex $[Ag(3ADMT)(NO_3)]_n$ was clarified on the basis of SC-XRD results that revealed a tetra-coordinated silver(I) center with two 3ADMT and two nitrate groups. The 1D polymer extension depends on the bridging nitrate and the argentophilic interaction. The supramolecular structure was analyzed qualitatively and quantitatively by utilizing Hirshfeld surface analysis. The percentage contributions of the most important contacts, O...H and N...H, are 37.2% and 18.8%, respectively. Biological evaluations indicated promising anticancer and antimicrobial properties of the $[Ag(3ADMT)(NO_3)]_n$ complex. The anticancer activities of the silver(I) complex are significantly greater than those of its free ligand, $AgNO_3$, and *cis*-platin against A-549 and MCF-7 cell lines. Based on MIC values and inhibition zone diameters, the Ag(I) complex has good potential towards both Gram-positive and Gram-negative bacteria and the

yeasts as well, but 3ADMT has no potential towards all examined microbes. Interestingly, the studied silver(I) complex has remarkable antibacterial potential against *P. vulgaris* (MIC = 6.1 μg/mL), which could be comparable to Gentamycin (MIC = 4.8 μg/mL). On the basis of the current results, we are motivated to carry out more studies on this fascinating class of compounds, which are promising anticancer candidates.

Supplementary Materials: The following supporting information can be downloaded at: https://www.mdpi.com/article/10.3390/inorganics11090350/s1, Figure S1: FTIR spectrum of the free ligand; 3ADMT; Figure S2: FTIR spectrum of the complex; $[Ag(3ADMT)(NO_3)]_n$; Table S1: Crystallographic details and crystal refinement parameters for the complex; Table S2: Evaluation of cytotoxicity against A-549 cell line for 3ADMT; Table S3: Evaluation of cytotoxicity against A-549 cell line for the complex $[Ag(3ADMT)(NO_3)]_n$; Table S4: Evaluation of cytotoxicity against MCF-7 cell line for 3ADMT; Table S5: Evaluation of cytotoxicity against MCF-7 cell line for $[Ag(3ADMT)(NO_3)]_n$; Method S1: Evaluation of cytotoxic effects against the two human lung (A-549) and breast (MCF-7) cancer cell lines; Method S2: Testing of antimicrobial activity.

Author Contributions: Conceptualization, M.A.M.A.-Y. and S.M.S.; methodology, M.A.E.-N.; software, M.H. and S.M.S.; validation, M.A.E.-N., A.B., and S.M.S.; formal analysis, M.A.E.-N. and M.H.; investigation, M.A.E.-N.; resources, A.B. and S.M.S.; data curation, S.M.S. writing—original draft preparation, M.A.E.-N., M.A.M.A.-Y., A.B., and S.M.S.; writing—review and editing, M.A.E.-N., M.A.M.A.-Y., M.H., A.B., and S.M.S.; supervision, M.A.M.A.-Y., M.M.S., and S.M.S.; project administration, M.A.E.-N., M.A.M.A.-Y., and S.M.S.; funding acquisition, A.B. All authors have read and agreed to the published version of the manuscript.

Funding: The authors would like to extend their sincere appreciation to the Researchers Supporting Project (RSP2023R64), King Saud University, Riyadh, Saudi Arabia.

Institutional Review Board Statement: Not applicable.

Data Availability Statement: Data is contained within the paper.

Acknowledgments: The authors would like to extend their sincere appreciation to the Researchers Supporting Project (RSP2023R64), King Saud University, Riyadh, Saudi Arabi.

Conflicts of Interest: The authors declare no conflict of interest.

References

1. Raju, S.K.; Karunakaran, A.; Kumar, S.; Sekar, P.; Murugesan, M.; Karthikeyan, M. Silver Complexes as Anticancer Agents: A Perspective Review. *Ger. J. Pharm. Biomater.* **2022**, *1*, 6–28. [CrossRef]
2. Tan, X.J.; Liu, H.Z.; Ye, C.Z.; Lou, J.F.; Liu, Y.; Xing, D.X.; Li, S.P.; Liu, S.L.; Song, L.Z. Synthesis, Characterization and in Vitro Cytotoxic Properties of New Silver(I) Complexes of Two Novel Schiff Bases Derived from Thiazole and Pyrazine. *Polyhedron* **2014**, *71*, 119–132. [CrossRef]
3. El-Naggar, M.A.; Abu-Youssef, M.A.M.; Soliman, S.M.; Haukka, M.; Al-Majid, A.M.; Barakat, A.; Badr, A.M.A. Synthesis, X-Ray Structure, Hirshfeld, and Antimicrobial Studies of New Ag(I) Complexes Based on Pyridine-Type Ligands. *J. Mol. Struct.* **2022**, *1264*, 133210. [CrossRef]
4. Altowyan, M.S.; El-Naggar, M.A.; Abu-Youssef, M.A.M.; Soliman, S.M.; Haukka, M.; Barakat, A.; Badr, A.M.A. Synthesis, X-Ray Structure, Antimicrobial and Anticancer Activity of a Novel $[Ag(Ethyl\text{-}3\text{-}Quinolate)_2(Citrate)]$ Complex. *Crystals* **2022**, *12*, 356. [CrossRef]
5. Nawaz, S.; Isab, A.A.; Merz, K.; Vasylyeva, V.; Metzler-Nolte, N.; Saleem, M.; Ahmad, S. Synthesis, Characterization and Antimicrobial Studies of Mixed Ligand Silver(I) Complexes of Triphenylphosphine and Heterocyclic Thiones: Crystal Structure of Bis[{(M2-Diazinane-2-Thione)(Diazinane-2-Thione)(Triphenylphosphine)Silver(I) Nitrate}]. *Polyhedron* **2011**, *30*, 1502–1506. [CrossRef]
6. Isab, A.A.; Nawaz, S.; Saleem, M.; Altaf, M.; Monim-ul-Mehboob, M.; Ahmad, S.; Evans, H.S. Synthesis, Characterization and Antimicrobial Studies of Mixed Ligand Silver(I) Complexes of Thioureas and Triphenylphosphine; Crystal Structure of $\{[Ag(PPh_3)(Thiourea)(NO_3)]_2 \cdot [Ag(PPh_3)(Thiourea)]_2(NO_3)_2\}$. *Polyhedron* **2010**, *29*, 1251–1256. [CrossRef]
7. Tan, S.J.; Yan, Y.K.; Lee, P.P.F.; Lim, K.H. Copper, Gold and Silver Compounds as Potential New Anti-Tumor Metallodrugs. *Future Med. Chem.* **2010**, *2*, 1591–1608. [CrossRef]
8. Nomiya, K.; Tsuda, K.; Sudoh, T.; Oda, M. Ag(I)-N bond-containing compound showing wide spectra in efective antimicrobial activities: Polymeric silver(I) imidazolate. *J. Inorg. Biochem.* **1997**, *68*, 39–44. [CrossRef]

9. El-Naggar, M.A.; Sharaf, M.M.; Albering, J.H.; Abu-Youssef, M.A.M.; Kassem, T.S.; Soliman, S.M.; Badr, A.M.A. One Pot Synthesis of Two Potent Ag(I) Complexes with Quinoxaline Ligand, X-Ray Structure, Hirshfeld Analysis, Antimicrobial, and Antitumor Investigations. *Sci. Rep.* **2022**, *12*, 1–14.
10. Abu-Youssef, M.A.M.; Soliman, S.M.; Langer, V.; Gohar, Y.M.; Hasanen, A.A.; Makhyoun, M.A.; Zaky, A.H.; Öhrström, L.R. Synthesis, Crystal Structure, Quantum Chemical Calculations, DNA Interactions, and Antimicrobial Activity of [Ag(2-Amino-3-Methylpyridine)$_2$]NO_3 and [Ag(Pyridine-2-Carboxaldoxime)NO_3]. *Inorg. Chem.* **2010**, *49*, 9788–9797. [CrossRef]
11. Spacciapoli, P.; Buxton, D.; Rothstein, D.; Friden, P. Antimicrobial Activity of Silver Nitrate against Periodontal Pathogens. *J. Periodontal Res.* **2001**, *36*, 108–113. [CrossRef] [PubMed]
12. Amin, M.; Glynn, F.; Phelan, S.; Sheahan, P.; Crotty, P.; McShane, D. Silver Nitrate Cauterisation, Does Concentration Matter? *Clin. Otolaryngol.* **2007**, *32*, 197–199. [PubMed]
13. De Gracia, C.G. An Open Study Comparing Topical Silver Sulfadiazine and Topical Silver Sulfadiazine-Cerium Nitrate in the Treatment of Moderate and Severe Burns. *Burns* **2001**, *27*, 67–74. [CrossRef] [PubMed]
14. Klasen, H.J. A Historical Review of the Use of Silver in the Treatment of Burns. II. Renewed Interest for Silver. *Burns* **2000**, *26*, 131–138. [CrossRef] [PubMed]
15. Mohan, M.; Gupta, S.K.; Kalra, V.K.; Vajpayee, R.B.; Sachdev, M.S. Topical Silver Sulphadiazine—A New Drug for Ocular Keratomycosis. *Br. J. Ophthalmol.* **1988**, *72*, 192–195. [CrossRef]
16. Eckhardt, S.; Brunetto, P.S.; Gagnon, J.; Priebe, M.; Giese, B.; Fromm, K.M. Nanobio Silver: Its Interactions with Peptides and Bacteria, and Its Uses in Medicine. *Chem. Rev.* **2013**, *113*, 4708–4754. [CrossRef]
17. Bayston, R.; Vera, L.; Mills, A.; Ashraf, W.; Stevenson, O.; Howdle, S.M. In Vitro Antimicrobial Activity of Silver-Processed Catheters for Neurosurgery. *J. Antimicrob. Chemother.* **2010**, *65*, 258–265. [CrossRef]
18. Fox, C.L.; Modak, S.M. Mechanism of Silver Sulfadiazine Action on Burn Wound Infections. *Antimicrob. Agents Chemother.* **1974**, *5*, 582–588. [CrossRef]
19. Feng, Q.L.; Wu, J.; Chen, G.Q.; Cui, F.Z.; Kim, T.N.; Kim, J.O.A. Mechanistic Study of the Antibacterial Effect of Silver Ions on Escherichia Coli and Staphylococcus Aureus. *J. Biomed. Mater. Res.* **2000**, *52*, 662–668. [CrossRef]
20. Irisli, S.; Tiryaki, F. Silver(I) Complexes Containing Diphosphine and Bis(Phosphine) Disulphide Ligands. *Asian J. Chem.* **2009**, *21*, 355–360.
21. Nomiya, K.; Noguchi, R.; Oda, M. Synthesis and Crystal Structure of Coinage Metal(I) Complexes with Tetrazole (Htetz) and Triphenylphosphine Ligands, and Their Antimicrobial Activities. A Helical Polymer of Silver(I) Complex [Ag(Tetz)$(PPh_3)_2]_n$ and a Monomeric Gold(I) Complex [Au(Tetz)(PPh_3)]. *Inorg. Chim. Acta* **2000**, *298*, 24–32.
22. Liu, H.; Long, S.; Rakesh, K.P.; Zha, G.F. Structure-Activity Relationships (SAR) of Triazine Derivatives: Promising Antimicrobial Agents. *Eur. J. Med. Chem.* **2020**, *185*, 111804. [CrossRef] [PubMed]
23. Singh, S.; Mandal, M.K.; Masih, A.; Saha, A.; Ghosh, S.K.; Bhat, H.R.; Singh, U.P. 1,3,5-Triazine: A Versatile Pharmacophore with Diverse Biological Activities. *Arch. Pharm.* **2021**, *354*, 2000363. [CrossRef]
24. Modh, R.P.; De Clercq, E.; Pannecouque, C.; Chikhalia, K.H. Design, Synthesis, Antimicrobial Activity and Anti-HIV Activity Evaluation of Novel Hybrid Quinazoline–Triazine Derivatives. *J. Enzyme Inhib. Med. Chem.* **2014**, *29*, 100–108. [CrossRef] [PubMed]
25. Kumar, A.; Srivastava, K.; Raja Kumar, S.; Puri, S.K.; Chauhan, P.M.S. Synthesis and Bioevaluation of Hybrid 4-Aminoquinoline Triazines as a New Class of Antimalarial Agents. *Bioorg. Med. Chem. Lett.* **2008**, *18*, 6530–6533. [CrossRef] [PubMed]
26. El-Gendy, Z.; Morsy, J.M.; Allimony, H.A.; Abdel-Monem, W.R.; Abdel-Rahman, R.M. Synthesis of Heterobicyclic Nitrogen Systems Bearing a 1,2,4-Triazine Moiety as Anticancer Drugs: Part IV. *Phosphorus Sulfur Silicon Relat. Elem.* **2006**, *178*, 2055–2071. [CrossRef]
27. Menicagli, R.; Samaritani, S.; Signore, G.; Vaglini, F.; Dalla Via, L. In Vitro Cytotoxic Activities of 2-Alkyl-4,6-Diheteroalkyl-1,3,5-Triazines: New Molecules in Anticancer Research. *J. Med. Chem.* **2004**, *47*, 4649–4652. [CrossRef]
28. Hunt, J.C.A.; Briggs, E.; Clarke, E.D.; Whittingham, W.G. Synthesis and SAR Studies of Novel Antifungal 1,2,3-Triazines. *Bioorg. Med. Chem. Lett.* **2007**, *17*, 5222–5226. [CrossRef]
29. Sangeetha, R.; Balasubramani, K.; Thanigaimani, K.; Razak, I.A. 6-Amino-3,4-Dimethyl-1,2,4-Triazin-1-Ium 2-Anilinobenzoate–3-Amino-5,6-Dimethyl-1,2,4-Triazine (1/1). *IUCrData* **2017**, *2*, x170829. [CrossRef]
30. Fathalla, E.M.; Abu-Youssef, M.A.M.; Sharaf, M.M.; El-Faham, A.; Barakat, A.; Badr, A.M.A.; Soliman, S.M.; Slawin, A.M.Z.; Woollins, J.D. Synthesis, Characterizations, Antitumor and Antimicrobial Evaluations of Novel Mn(II) and Cu(II) Complexes with NNN-Tridentate s-Triazine-Schiff Base Ligand. *Inorg. Chim. Acta* **2023**, *555*, 121586. [CrossRef]
31. Yousri, A.; El-Faham, A.; Haukka, M.; Ayoup, M.S.; Ismail, M.M.F.; Menofy, N.G.E.; Soliman, S.M.; Öhrström, L.; Barakat, A.; Abu-Youssef, M.A.M. A Novel Na(I) Coordination Complex with s-Triazine Pincer Ligand: Synthesis, X-Ray Structure, Hirshfeld Analysis, and Antimicrobial Activity. *Crystals* **2023**, *13*, 890. [CrossRef]
32. Ismail, A.M.; El Sayed, S.A.; Butler, I.S.; Mostafa, S.I. New Palladium(II), Platinum(II) and Silver(I) Complexes of 2-Amino-4,6-Dithio-1,3,5-Triazine; Synthesis, Characterization and DNA Binding Properties. *J. Mol. Struct.* **2020**, *1200*, 127088. [CrossRef]

33. El-Naggar, M.A.; Albering, J.H.; Barakat, A.; Abu-Youssef, M.A.M.; Soliman, S.M.; Badr, A.M.A. New Bioactive 1D Ag(I) Coordination Polymers with Pyrazole and Triazine Ligands; Synthesis, X-Ray Structure, Hirshfeld Analysis and DFT Studies. *Inorg. Chim. Acta* **2022**, *537*, 120948. [CrossRef]
34. Almalioti, F.; MacDougall, J.; Hughes, S.; Hasson, M.M.; Jenkins, R.L.; Ward, B.D.; Tizzard, G.J.; Coles, S.J.; Williams, D.W.; Bamford, S.; et al. Convenient Syntheses of Cyanuric Chloride-Derived NHC Ligands, Their Ag(I) and Au(I) Complexes and Antimicrobial Activity. *Dalton Trans.* **2013**, *42*, 12370–12380. [CrossRef] [PubMed]
35. Swamy, S.J.; Reddy, E.R.; Raju, D.N.; Jyothi, S. Synthesis and Spectral Investigations of Manganese(II), Cobalt(II), Nickel(II), Copper(II) and Zinc(II) Complexes of New Polydentate Ligands Containing a 1,8-Naphthyridine Moiety. *Molecules* **2006**, *11*, 1000–1008. [CrossRef]
36. Raman, N.; Dhaveethu Raja, J.; Sakthivel, A. Synthesis, Spectral Characterization of Schiff Base Transition Metal Complexes: DNA Cleavage and Antimicrobial Activity Studies. *J. Chem. Sci.* **2007**, *119*, 303–310. [CrossRef]
37. Mohamed, M.S.; Shoukry, A.A.; Ali, A.G. Synthesis and Structural Characterization of Ternary Cu (II) Complexes of Glycine with 2,2′-Bipyridine and 2,2′-Dipyridylamine. The DNA-Binding Studies and Biological Activity. *Spectrochim. Acta Part A Mol. Biomol. Spectrosc.* **2012**, *86*, 562–570. [CrossRef]
38. Sharkey, M.A.; O'Gara, J.P.; Gordon, S.V.; Hackenberg, F.; Healy, C.; Paradisi, F.; Patil, S.; Schaible, B.; Tacke, M. Investigations into the Antibacterial Activity of the Silver-Based Antibiotic Drug Candidate SBC3. *Antibiotics* **2012**, *1*, 25–28. [CrossRef]
39. Schmidbaur, H.; Schier, A. Argentophilic interactions. *Angew Chem.—Int. Ed.* **2015**, *54*, 746–784. [CrossRef]
40. Jiang, Y.H.; Cui, L.N.; Huang, X.; Jin, Q.H.; Zhang, C.L. Tris(3-amino-5,6-dimethyl-1,2,4-triazine-Nκ2)silver(I) trifluromethanesulfonate-3-amino-5,6-dimethyl-1,2,4-triazine (1/1). *Acta Crystallogr. E Crystallogr. Commun.* **2011**, *67*, m1526–m1527.
41. Clausen, H.F.; Chevallier, M.S.; Spackman, M.A.; Iversen, B.B. Three New Co-Crystals of Hydroquinone: Crystal Structures and Hirshfeld Surface Analysis of Intermolecular Interactions. *N. J. Chem.* **2010**, *34*, 193–199. [CrossRef]
42. Spackman, M.A.; Byrom, P.G. A Novel Definition of a Molecule in a Crystal. *Chem. Phys. Lett.* **1997**, *267*, 215–220. [CrossRef]
43. McKinnon, J.J.; Spackman, M.A.; Mitchell, A.S. Novel Tools for Visualizing and Exploring Intermolecular Interactions in Molecular Crystals. *Acta Crystallogr. B Struct. Sci. Cryst. Eng. Mater.* **2004**, *60*, 627–668. [CrossRef]
44. McKinnon, J.J.; Jayatilaka, D.; Spackman, M.A. Towards Quantitative Analysis of Intermolecular Interactions with Hirshfeld Surfaces. *Chem. Commun.* **2007**, *37*, 3814–3816. [CrossRef] [PubMed]
45. Lippert, B. *Cisplatin: Chemistry and Biochemistry of a Leading Anticancer Drug*; Verlag Helvetica Chimica Acta: Zürich, Switzerland, 1999.
46. Adams, M.; Kerby, I.J.; Rocker, I.; Evans, A.; Johansen, K.; Franks, C.R. A Comparison of the Toxicity and Efficacy of Cisplatin and Carboplatin in Advanced Ovarian Cancer. *Acta Oncol.* **2009**, *28*, 57–60. [CrossRef] [PubMed]
47. Oun, R.; Moussa, Y.E.; Wheate, N.J. The Side Effects of Platinum-Based Chemotherapy Drugs: A Review for Chemists. *Dalton Trans.* **2018**, *47*, 6645–6653. [CrossRef]
48. Piccart, M.J.; Lamb, H.; Vermorken, J.B. Current and Future Potential Roles of the Platinum Drugs in the Treatment of Ovarian Cancer. *Ann. Oncol.* **2001**, *12*, 1195–1203. [CrossRef]
49. Zhang, Q.L.; Liu, J.G.; Liu, J.; Xue, G.Q.; Li, H.; Liu, J.Z.; Zhou, H.; Qu, L.H.; Ji, L.N. DNA-Binding and Photocleavage Studies of Cobalt(III) Mixed-Polypyridyl Complexes Containing 2-(2-Chloro-5-Nitrophenyl)Imidazo [4,5-f][1,10]Phenanthroline. *J. Inorg. Biochem.* **2001**, *85*, 291–296. [CrossRef]
50. Puszyńska-Tuszkanow, M.; Grabowski, T.; Daszkiewicz, M.; Wietrzyk, J.; Filip, B.; MacIejewska, G.; Cieślak-Golonka, M. Silver(I) Complexes with Hydantoins and Allantoin: Synthesis, Crystal and Molecular Structure, Cytotoxicity and Pharmacokinetics. *J. Inorg. Biochem.* **2011**, *105*, 17–22. [CrossRef]
51. Medici, S.; Peana, M.; Nurchi, V.M.; Lachowicz, J.I.; Crisponi, G.; Zoroddu, M.A. Noble Metals in Medicine: Latest Advances. *Coord. Chem. Rev.* **2015**, *284*, 329–350. [CrossRef]
52. Zaki, M.; Arjmand, F.; Tabassum, S. Current and Future Potential of Metallo Drugs: Revisiting DNA-Binding of Metal Containing Molecules and Their Diverse Mechanism of Action. *Inorg. Chim. Acta* **2016**, *444*, 1–22. [CrossRef]
53. Banti, C.N.; Hadjikakou, S.K. Anti-Proliferative and Anti-Tumor Activity of Silver(I) Compounds. *Metallomics* **2013**, *5*, 569–596. [CrossRef] [PubMed]
54. Ali, K.A.; Abd-Elzaher, M.M.; Mahmoud, K. Synthesis and Anticancer Properties of Silver(I) Complexes Containing 2,6-Bis(Substituted)Pyridine Derivatives. *Int. J. Med. Chem.* **2013**, *2013*, 256836. [CrossRef]
55. Medici, S.; Peana, M.; Crisponi, G.; Nurchi, V.M.; Lachowicz, J.I.; Remelli, M.; Zoroddu, M.A. Silver Coordination Compounds: A New Horizon in Medicine. *Coord. Chem. Rev.* **2016**, *327*, 349–359. [CrossRef]
56. Yousri, A.; Haukka, M.; Abu-Youssef, M.A.; Ayoup, M.S.; Ismail, M.M.; El Menofy, N.G.; Soliman, S.M.; Barakat, A.; Noa, F.M.A.; Öhrström, L. Synthesis, structure diversity, and antimicrobial studies of Ag (I) complexes with quinoline-type ligands. *Cryst. Eng. Comm.* **2023**, *25*, 3922–3930. [CrossRef]
57. Rigaku Oxford Diffraction. *CrysAlisPro*; Agilent Technologies Inc.: Oxfordshire, UK, 2020.
58. Sheldrick, G.M. Shelxt–integrated space-group and crystal-structure determination. *Acta Cryst.* **2015**, *A71*, 3–8. [CrossRef]
59. Sheldrick, G.M. Crystal structure refinement with *SHELXL*. *Acta Cryst.* **2015**, *C71*, 3–8.
60. Hübschle, C.B.; Sheldrick, G.M.; Dittrich, B. ShelXle: A Qt graphical user interface for SHELXL. *J. Appl. Cryst.* **2011**, *44*, 1281–1284. [CrossRef]

61. Spackman, M.A.; Jayatilaka, D. Hirshfeld Surface Analysis. *Cryst. Eng. Comm.* **2009**, *11*, 19–32. [CrossRef]
62. Mosmann, T. Rapid Colorimetric Assay for Cellular Growth and Survival: Application to Proliferation and Cytotoxicity Assays. *J. Immunol. Methods* **1983**, *65*, 55–63. [CrossRef]

Disclaimer/Publisher's Note: The statements, opinions and data contained in all publications are solely those of the individual author(s) and contributor(s) and not of MDPI and/or the editor(s). MDPI and/or the editor(s) disclaim responsibility for any injury to people or property resulting from any ideas, methods, instructions or products referred to in the content.